2023 62nd IEEE Conference on Decision and Control (CDC)
December 13-15, 2023. Marina Bay Sands, Singapore

Design of Limit-Cycle Oscillators with Prescribed Trajectories and Phase-Response Properties via Phase Reduction and Floquet Theory

Norihisa Namura and Hiroya Nakao

***Abstract*— We propose a method for designing stable limit-cycle oscillators with prescribed periodic trajectories and phase-response properties in general dimensions based on the phase reduction theory. The vector field of the oscillator is approximated by polynomials and their coefficients are optimized to satisfy required conditions. Linear stability of the periodic trajectory is ensured by imposing conditions on the eigenvalues of the monodromy matrix based on Floquet theory. We verify the validity of the proposed method by designing several types of oscillators with given properties. As an application, we design two oscillators with the same periodic trajectory but with different phase-response properties and show their distinct synchronization dynamics under the same periodic input.**

I. INTRODUCTION

Synchronization of rhythmic systems has been widely applied in various fields of engineering in recent years. Some examples include human-robot interactions [1], power networks [2], frequency tuning or stabilization in electrical oscillators [3], and suppression of pulsus alternans in the heart [4]. Limit-cycle oscillators, i.e., nonlinear dynamical systems with stable limit-cycle trajectories, provide a typical mathematical model of rhythmic systems [5]. When a periodic input is given to a limit-cycle oscillator, *entrainment* or *phase locking* of the oscillator to the periodic input can be observed [6], [7]. When two or more oscillators interact, mutual synchronization of the oscillators can be observed.

The phase reduction theory [6], [8], [9], [10], [11], [12], [13], which approximately describes the multidimensional dynamics of a limit-cycle oscillator by a one-dimensional phase equation using only the phase value defined along the limit cycle, is useful for analyzing synchronization dynamics of limit-cycle oscillators subjected to weak inputs. The phase reduction theory has been extensively used for analyzing various types of synchronization dynamics of limit-cycle oscillators [6], [9], [12], [14]. Recently, it has also been applied to the synchronization control of limit-cycle oscillators [15], [16], [17], [18], [19], [20], [21].

In controlling rhythmic dynamical behaviors of artificial objects, e.g., in robotics [22], [23], it is important to design limit-cycle oscillators with desired non-intersecting periodic trajectories. Many studies have been conducted on the design of oscillators with prescribed periodic trajectories [22], [24], [25]. In particular, several methods have been proposed to design dynamical systems with stable limit cycles of given shapes by constructing the vector fields [26], [27], [28]. Design of limit cycle oscillators using neural networks has also been considered [29], [30], [31]. For applications to synchronization control, it is also important to design oscillators with desired phase-response properties that determine the synchronization characteristics in addition to the desired trajectories. However, few studies have considered the phase-response properties explicitly. In our previous study [28], we proposed a method for designing stable limit-cycle oscillators with prescribed trajectories and phase-response properties, but it was valid only in two-dimensional cases.

In this study, we propose an extension of our previous study [28] to multidimensional cases. As in [28], we approximate the vector field of the oscillator by using polynomials and optimize their coefficients. For ensuring the linear stability of the limit cycle, we evaluate the eigenvalues of the monodromy matrix along the periodic trajectory according to Floquet theory [32], [33], in contrast to [28]. We verify the validity of the proposed method numerically by designing several types of oscillators. As an application, we design two oscillators with the same periodic trajectory but with different phase-response properties and show their distinct synchronization characteristics under the same input.

This paper is organized as follows. We first describe phase reduction in Sec. II and Floquet theory in Sec. III, respectively. We then describe the method for designing the vector field of oscillators in Sec. IV. In Sec. V, we verify the proposed method by numerical simulations for several types of oscillators and demonstrate the importance of the phase-response properties. We conclude this study in Sec. VI.

II. PHASE REDUCTION AND SYNCHRONIZATION

In this section, we explain the phase reduction theory for analyzing synchronization [6], [8], [9], [10], [11], [12], [13].

A. Phase Reduction with Weak Periodic Inputs

We consider a limit-cycle oscillator described by

$$\dot{\boldsymbol{X}} = \boldsymbol{F}(\boldsymbol{X}), \tag{1}$$

where $\boldsymbol{X}(t) \in \mathbb{R}^N$ is the system state at time t, $\boldsymbol{F} : \mathbb{R}^N \to \mathbb{R}^N$ is a smooth vector field, and $\dot{\boldsymbol{X}}$ is the time derivative of $\boldsymbol{X}$. We assume that the system has an exponentially stable limit-cycle solution $\tilde{\boldsymbol{X}}_0(t)$ with a natural period T and frequency $\omega = 2\pi/T$, which is a T-periodic function of t satisfying $\tilde{\boldsymbol{X}}_0(t+T) = \tilde{\boldsymbol{X}}_0(t)$.

N. Namura is with the Department of Systems and Control Engineering, Tokyo Institute of Technology, Tokyo, Japan namura.n.aa@m.titech.ac.jp

H. Nakao is with the Department of Systems and Control Engineering, Tokyo Institute of Technology, Tokyo, Japan nakao@sc.e.titech.ac.jp

This work was supported in part by JSPS KAKENHI JP22K11919, JP22H00516, and JST CREST JP-MJCR1913.

We first introduce the asymptotic phase function $\Theta : \mathcal{B} \to [0, 2\pi)$ for the limit-cycle oscillator described by $\dot{\boldsymbol{X}} = \boldsymbol{F}(\boldsymbol{X})$ in the whole basin $\mathcal{B}$ of the limit cycle so that it satisfies $\langle \nabla\Theta(\boldsymbol{X}), \boldsymbol{F}(\boldsymbol{X})\rangle = \omega$. Here, $\langle \boldsymbol{a}, \boldsymbol{c}\rangle = \sum_{j=1}^{N} a_j^* c_j : \mathbb{C}^N \times \mathbb{C}^N \to \mathbb{C}$ represents the scalar product of two complex vectors $\boldsymbol{a}, \boldsymbol{c} \in \mathbb{C}^N$, where $*$ denotes the complex conjugate. Using the asymptotic phase, we can define the phase value θ of the state $\boldsymbol{X} \in \mathcal{B}$ by $\theta = \Theta(\boldsymbol{X})$. This phase value increases constantly at the frequency ω as

$$\dot{\theta}(t) = \dot{\Theta}(\boldsymbol{X}(t)) = \langle \nabla\Theta(\boldsymbol{X}(t)), \boldsymbol{F}(\boldsymbol{X}(t))\rangle = \omega. \quad (2)$$

Here, the phase values 0 and 2π are considered identical. The state of the oscillator on the limit cycle can be expressed as $\boldsymbol{X}_0(\theta) = \tilde{\boldsymbol{X}}_0(t = \theta/\omega)$ as a function of the phase θ, where $\boldsymbol{X}_0(\theta)$ is a function of period 2π (i.e., $\boldsymbol{X}_0(\theta) = \boldsymbol{X}_0(\theta+2\pi)$).

We next consider the case that the limit-cycle oscillator is perturbed by a sufficiently weak input as

$$\dot{\boldsymbol{X}}(t) = \boldsymbol{F}(\boldsymbol{X}(t)) + \varepsilon \boldsymbol{q}(t), \quad (3)$$

where $\boldsymbol{q}(t)$ represents a periodic input with a period τ and frequency $\Omega = 2\pi/\tau$ satisfying $\boldsymbol{q}(t + \tau) = \boldsymbol{q}(t)$ and the non-dimensional parameter $0 < \varepsilon \ll 1$ characterizes the strength of the input. Since ε is assumed sufficiently small, the deviation of the oscillator state $\boldsymbol{X}(t)$ from the state $\boldsymbol{X}_0(\theta(t))$ on the limit cycle is of $O(\varepsilon)$, i.e.,

$$\boldsymbol{X}(t) = \boldsymbol{X}_0(\theta(t)) + O(\varepsilon). \quad (4)$$

Substituting Eq. (4) into Eq. (3) and ignoring errors of $O(\varepsilon^2)$, we can obtain the time evolution of the phase $\theta(t)$ as

$$\dot{\theta}(t) = \omega + \varepsilon \langle \boldsymbol{Z}(\theta(t)), \boldsymbol{q}(t)\rangle . \quad (5)$$

Here, $\boldsymbol{Z} : [0, 2\pi) \to \mathbb{R}^N$ is the phase sensitivity function (PSF, also known as the infinitesimal phase resetting curve, iPRC), which is defined by the gradient of the phase function at $\boldsymbol{X}_0(\theta)$ on the limit cycle as $\boldsymbol{Z}(\theta) = \nabla\Theta(\boldsymbol{X})|_{\boldsymbol{X}=\boldsymbol{X}_0(\theta)}$. The PSF describes linear phase-response properties of the oscillator caused by weak inputs [6], [9], [10], [11], [12].

Our aim in this study is to develop a method to design limit-cycle oscillators with prescribed periodic trajectories and phase-response properties characterized by the PSF.

B. Synchronization

We next analyze synchronization of the oscillator with a weak periodic input by using the averaging approximation [6], [8], [12]. Assuming that the natural frequency ω of the oscillator and the frequency Ω of the periodic input are sufficiently close because of the weakness of the input, we denote the frequency difference by $\varepsilon\Delta = \omega - \Omega$ using the small parameter ε and a parameter Δ of $O(1)$, where "$\varepsilon\Delta$" indicates that the frequency difference is of $O(\varepsilon)$. The oscillator phase relative to the input, $\phi(t) = \theta(t) - \Omega t$, obeys

$$\dot{\phi}(t) = \varepsilon \left(\Delta + \langle \boldsymbol{Z}(\phi(t) + \Omega t), \boldsymbol{q}(t)\rangle\right), \quad (6)$$

where the range of ϕ is extended outside $[0, 2\pi)$ and $\boldsymbol{Z}$ is regarded as a 2π-periodic function. Since the right-hand side is of $O(\varepsilon)$ and ϕ is a slow variable, we can perform averaging approximation [6], [8], [12]. Averaging the right-hand side of Eq. (6) over one period of the input while fixing $\phi(t)$ yields a single-variable autonomous system,

$$\dot{\phi} = \varepsilon \left(\Delta + \Gamma(\phi)\right). \quad (7)$$

Here, $\Gamma(\phi)$ is a 2π-periodic phase coupling function (PCF)

$$\Gamma(\phi) = \frac{1}{2\pi} \int_0^{2\pi} \langle \boldsymbol{Z}(\phi + \psi), \boldsymbol{q}\left(\psi/\Omega\right)\rangle \, d\psi, \quad (8)$$

where $\psi = \Omega t$ is the phase of the input.

If the time derivative of the phase difference is zero, $\dot{\phi} = 0$, the oscillator is entrained to the periodic input. The phase-locking point ϕ_0 is stable if it satisfies the phase-locking condition $\Delta + \Gamma(\phi_0) = 0$ and stability condition $\Gamma'(\phi_0) < 0$, where $\Gamma'(\phi)$ is the derivative of $\Gamma(\phi)$ by ϕ.

III. FLOQUET THEORY

The linear stability of the limit cycle can be analyzed by Floquet theory [32], [33]. We assume that the oscillator state $\boldsymbol{X}(t)$ is near the limit cycle $\tilde{\boldsymbol{X}}_0(t)$ and can be described as $\boldsymbol{X}(t) = \tilde{\boldsymbol{X}}_0(t) + \varepsilon \boldsymbol{y}(t)$, where the deviation is $O(\varepsilon)$ as in Eq. (4). The variation $\boldsymbol{y}(t)$ approximately obeys the following linearized periodic system:

$$\dot{\boldsymbol{y}}(t) = \tilde{\boldsymbol{J}}(t)\boldsymbol{y}(t), \quad (9)$$

where $\tilde{\boldsymbol{J}}(t)$ is the Jacobian matrix of $\boldsymbol{F}$ evaluated at $\boldsymbol{X}_0(\theta(t))$ on the limit cycle.

We define the fundamental matrix of the linearized system (9) by $\boldsymbol{V} \in \mathbb{R}^{N\times N}$, which is a regular matrix satisfying $\dot{\boldsymbol{V}}(t) = \tilde{\boldsymbol{J}}(t)\boldsymbol{V}(t)$. We can define a regular and constant matrix $\boldsymbol{M} \in \mathbb{R}^{N\times N}$ satisfying $\boldsymbol{V}(T) = \boldsymbol{V}(0)\boldsymbol{M}$, where $\boldsymbol{M}$ is called a monodromy matrix and depends on the initial condition $\tilde{\boldsymbol{X}}_0(0)$. Since $\boldsymbol{M}$ is regular, there exists a matrix $\boldsymbol{\Lambda} \in \mathbb{C}^{N\times N}$ such that $\boldsymbol{M} = \exp(\boldsymbol{\Lambda}T)$. From Floquet theory, the fundamental matrix can be expressed as

$$\boldsymbol{V}(t) = \boldsymbol{R}(t) \exp(\boldsymbol{\Lambda}t), \quad (10)$$

where $\boldsymbol{R}(t) \in \mathbb{C}^{N\times N}$ is a T-periodic regular matrix satisfying $\boldsymbol{R}(t + T) = \boldsymbol{R}(t)$ and $\boldsymbol{R}(0) = \boldsymbol{I}$, i.e., $\boldsymbol{V}(0) = \boldsymbol{I}$, where $\boldsymbol{I}$ is the identity matrix. Since $\boldsymbol{R}(t)$ is T-periodic, the eigenvalues of $\boldsymbol{\Lambda}$ characterize the stability.

Though the monodromy matrix $\boldsymbol{M}$ depends on the initial condition, the eigenvalues of $\boldsymbol{M}$ are uniquely determined because eigenvalues are invariant under similarity transformation, so we can obtain the eigenvalues of $\boldsymbol{M}$ by simply calculating $\boldsymbol{V}(T)$ assuming $\boldsymbol{V}(0) = \boldsymbol{I}$.

We next consider the eigensystem of $\boldsymbol{\Lambda}$: $\left\{\lambda_j \in \mathbb{C},\ \boldsymbol{u}_j \in \mathbb{C}^N, \boldsymbol{v}_j \in \mathbb{C}^N\right\}_{j=1}^{N}$, where $\boldsymbol{\Lambda}_j\boldsymbol{u}_j = \lambda_j\boldsymbol{u}_j$ and $\boldsymbol{\Lambda}_j^\dagger\boldsymbol{v}_j = \lambda_j^\dagger\boldsymbol{v}_j$ ($\dagger$ denotes the Hermitian conjugate). The eigenvalue λ_j is called Floquet exponent (i.e., $\exp(\lambda_j T)$ is the Floquet multiplier), where the principal value is chosen for complex λ_j. The exponents $\{\lambda_j\}$ are sorted as $\mathrm{Re}\ \lambda_1 \geq \cdots \geq \mathrm{Re}\ \lambda_N$. For a stable limit cycle, $\lambda_1 = 0$ holds. The eigenvectors $\boldsymbol{u}_k$ and $\boldsymbol{v}_j$ can be bi-orthonormalized to satisfy $\langle \boldsymbol{v}_j, \boldsymbol{u}_k\rangle = \delta_{jk}$ for $j, k = 1, \ldots, N$.

We further define the time evolution of $\boldsymbol{u}_j$ and $\boldsymbol{v}_j$ by $\boldsymbol{u}_j(t) = \boldsymbol{R}(t)\boldsymbol{u}_j$ and $\boldsymbol{v}_j(t) = \left(\boldsymbol{R}(t)^\dagger\right)^{-1}\boldsymbol{v}_j$ for $0 \leq t < T$, where we call $\boldsymbol{u}_j(t)$ and $\boldsymbol{v}_j(t)$ the right and left Floquet vectors, respectively. These vectors are T-periodic and satisfy $\boldsymbol{u}_j(T) = \boldsymbol{u}_j(0) = \boldsymbol{u}_j$, $\boldsymbol{v}_j(T) = \boldsymbol{v}_j(0) = \boldsymbol{v}_j$, and bi-orthonormality condition $\langle \boldsymbol{v}_j(t), \boldsymbol{u}_k(t)\rangle = \delta_{jk}$ for all $0 \leq t < T$. They are T-periodic solution to the following linear system and its adjoint, respectively [13], [21]:

$$\dot{\boldsymbol{u}}_j(t) = \left[\tilde{\boldsymbol{J}}(t) - \lambda_j\right]\boldsymbol{u}_j(t), \tag{11}$$

$$\dot{\boldsymbol{v}}_j(t) = -\left[\tilde{\boldsymbol{J}}(t)^\dagger - \lambda_j^\dagger\right]\boldsymbol{v}_j(t). \tag{12}$$

If we take $\boldsymbol{u}_1(0) = \frac{1}{\omega}\boldsymbol{F}(\tilde{\boldsymbol{X}}_0(0))$, $\boldsymbol{Z}(\theta(t)) = \boldsymbol{v}(t)$ holds, so we consider the PSF as a function of t as $\tilde{\boldsymbol{Z}}(t) \coloneqq \boldsymbol{Z}(\theta(t))$. It is known that $\tilde{\boldsymbol{Z}}(t)$ obeys the following adjoint equation (13) and normalization condition (14) [10], [11]:

$$\dot{\tilde{\boldsymbol{Z}}}(t) = -\tilde{\boldsymbol{J}}^\top(t)\tilde{\boldsymbol{Z}}(t), \tag{13}$$

$$\left\langle \tilde{\boldsymbol{Z}}(t), \dot{\tilde{\boldsymbol{X}}}_0(t)\right\rangle = \omega. \tag{14}$$

IV. DESIGN METHOD FOR VECTOR FIELDS

In this section, we propose a method for designing a stable limit-cycle oscillator with a given trajectory and PSF.

A. Conditions for the Periodic Trajectory and PSF

We extend our previous method [28] to N-dimensional systems. We approximate the vector field of the system by using polynomials of order n as

$$\boldsymbol{F}(\boldsymbol{X}) = \begin{bmatrix} F_1(\boldsymbol{X}) \\ \vdots \\ F_N(\boldsymbol{X}) \end{bmatrix} \simeq \begin{bmatrix} \boldsymbol{U}(\boldsymbol{X})^\top\boldsymbol{\zeta}_1 \\ \vdots \\ \boldsymbol{U}(\boldsymbol{X})^\top\boldsymbol{\zeta}_N \end{bmatrix}, \tag{15}$$

where $\boldsymbol{X} = [x_1 \ \cdots \ x_N]$, $\boldsymbol{U}(\boldsymbol{X}) \in \mathbb{R}^P$ is given by

$$\begin{aligned}&\boldsymbol{U}(\boldsymbol{X}) \\ &= \begin{bmatrix} 1 & \overline{x_1} & \cdots & \overline{x_N} & \overline{x_1^2} & \overline{x_1x_2} & \cdots & \overline{x_N^2} & \cdots & \overline{x_N^n}, \end{bmatrix}^\top,\end{aligned} \tag{16}$$

and $\boldsymbol{\zeta}_1, \ldots, \boldsymbol{\zeta}_N \in \mathbb{R}^P$ are the coefficient vectors. Here, the overline denotes standardization, $\overline{z} \coloneqq (z-\mu)/\sigma$, where μ and σ are the mean and standard deviation of z, respectively.

We assume that the system has a non-intersecting differentiable periodic trajectory $\boldsymbol{p}(t) = [p_1(t) \cdots p_N(t)]^\top$ and impose the following condition on the vector field:

$$\dot{\boldsymbol{p}} = \boldsymbol{F}(\boldsymbol{p}), \tag{17}$$

which can be expressed in the polynomial approximation as $\boldsymbol{U}(\boldsymbol{p}(t))^\top\boldsymbol{\zeta}_j \simeq \dot{p}_j(t)$ for $j = 1, \ldots, N$.

We introduce a coefficient vector $\boldsymbol{\xi} = \left[\boldsymbol{\zeta}_1^\top \ \cdots \ \boldsymbol{\zeta}_N^\top\right]^\top \in \mathbb{R}^{NP}$ and discretize the time t using L points as $t_\ell = (\ell-1)\Delta t$, where $\ell = 1, \ldots, L$ and Δt is the time interval. Defining $\boldsymbol{A}_{\boldsymbol{p},\ell} \in \mathbb{R}^{N\times NP}$ and $\boldsymbol{b}_{\boldsymbol{p},\ell} \in \mathbb{R}^N$ by

$$\boldsymbol{A}_{\boldsymbol{p},\ell} \coloneqq \begin{bmatrix} \boldsymbol{U}(\boldsymbol{p}(t_\ell))^\top & \cdots & \boldsymbol{0} \\ \vdots & \ddots & \vdots \\ \boldsymbol{0} & \cdots & \boldsymbol{U}(\boldsymbol{p}(t_\ell))^\top \end{bmatrix}, \tag{18}$$

$$\boldsymbol{b}_{\boldsymbol{p},\ell}^\top \coloneqq \begin{bmatrix} \dot{p}_1(t_\ell) & \cdots & \dot{p}_N(t_\ell) \end{bmatrix}^\top \tag{19}$$

for each t_ℓ, respectively, we can express the discrepancy of the polynomial approximation from Eq. (17) as $\boldsymbol{A}_{\boldsymbol{p},\ell}\boldsymbol{\xi} - \boldsymbol{b}_{\boldsymbol{p},\ell}$.

Next, we introduce the conditions for the PSF to the vector field. We note that the periodic trajectory and PSF are not completely independent because they should satisfy the normalization condition (14). Assuming that the oscillator has a PSF $\tilde{\boldsymbol{Z}}(t) = [\tilde{\boldsymbol{Z}}_1(t) \ \cdots \ \tilde{\boldsymbol{Z}}_N(t)]^\top$, we require that the adjoint equation (13) is satisfied. This equation is expressed in the polynomial approximation as

$$\tilde{Z}_1(t)\boldsymbol{U}_j(\boldsymbol{p}(t))^\top\boldsymbol{\zeta}_1 + \cdots + \tilde{Z}_N(t)\boldsymbol{U}_j(\boldsymbol{p}(t))^\top\boldsymbol{\zeta}_N \simeq -\dot{\tilde{Z}}_j(t), \tag{20}$$

for $j = 1, \ldots, N$, where $\boldsymbol{U}_j(\boldsymbol{X}) \in \mathbb{R}^P$ is the jth column of $\nabla\boldsymbol{U}(\boldsymbol{X})$. Defining $\boldsymbol{A}_{\boldsymbol{Z},\ell} \in \mathbb{R}^{N\times NP}$ and $\boldsymbol{b}_{\boldsymbol{Z},\ell} \in \mathbb{R}^N$ by

$$\boldsymbol{A}_{\boldsymbol{Z},\ell} \coloneqq \begin{bmatrix} \tilde{Z}_1(t_\ell)\boldsymbol{U}_1(\boldsymbol{p}(t_\ell))^\top & \cdots & \tilde{Z}_N(t_\ell)\boldsymbol{U}_1(\boldsymbol{p}(t_\ell))^\top \\ \vdots & \ddots & \vdots \\ \tilde{Z}_1(t_\ell)\boldsymbol{U}_N(\boldsymbol{p}(t_\ell))^\top & \cdots & \tilde{Z}_N(t_\ell)\boldsymbol{U}_N(\boldsymbol{p}(t_\ell))^\top \end{bmatrix}, \tag{21}$$

$$\boldsymbol{b}_{\boldsymbol{Z},\ell}^\top \coloneqq \begin{bmatrix} -\dot{\tilde{Z}}_1(t_\ell) & \cdots & -\dot{\tilde{Z}}_N(t_\ell) \end{bmatrix}^\top, \tag{22}$$

respectively, we can express the discrepancy of the polynomial approximation from Eq. (13) as $\boldsymbol{A}_{\boldsymbol{Z},\ell}\boldsymbol{\xi} - \boldsymbol{b}_{\boldsymbol{Z},\ell}$.

We seek the optimal coefficients of polynomials that satisfy Eqs. (17) and (13) as much as possible by minimizing the overall discrepancies of the periodic trajectory and PSF over one period T. Defining $\boldsymbol{A} \in \mathbb{R}^{2NL\times NP}$

$$\boldsymbol{A} = \begin{bmatrix} \boldsymbol{A}_{\boldsymbol{p},1}^\top & \cdots & \boldsymbol{A}_{\boldsymbol{p},L}^\top & \boldsymbol{A}_{\boldsymbol{Z},1}^\top & \cdots & \boldsymbol{A}_{\boldsymbol{Z},L}^\top \end{bmatrix}^\top \tag{23}$$

and $\boldsymbol{b} \in \mathbb{R}^{2NL}$ by

$$\boldsymbol{b} = \begin{bmatrix} \boldsymbol{b}_{\boldsymbol{p},1}^\top & \cdots & \boldsymbol{b}_{\boldsymbol{p},L}^\top & \boldsymbol{b}_{\boldsymbol{Z},1}^\top & \cdots & \boldsymbol{b}_{\boldsymbol{Z},L}^\top \end{bmatrix}^\top, \tag{24}$$

the sum of the squared errors for $\boldsymbol{p}$ and $\boldsymbol{Z}$ can be expressed as $\|\boldsymbol{A}\boldsymbol{\xi} - \boldsymbol{b}\|^2$. Finally, the objective function

$$E = \frac{1}{2}\left(\|\boldsymbol{A}\boldsymbol{\xi} - \boldsymbol{b}\|^2 + \gamma\|\boldsymbol{\xi}\|^2\right) \tag{25}$$

is obtained. Here, we add the regularization term $\|\boldsymbol{\xi}\|^2$ with the weight γ to prevent the coefficients of the vector field from becoming excessively large, which is expected to reduce the complexity of the vector field and ensures the uniqueness of the solution to the optimization problem.

B. Condition for the Linear Stability

To ensure the linear stability of the limit cycle, one of the Floquet exponents should be zero while the others should be negative. Therefore, we impose the conditions on them as follows:

$$\lambda_1 = 0, \tag{26}$$

$$\mathrm{Re}\ \lambda_j \leq \lambda_{\mathrm{tol}}, \quad j = 2, \ldots, N, \tag{27}$$

where $\lambda_{\mathrm{tol}} < 0$ is the maximum tolerance value of the Floquet exponents. Since the Floquet exponents are obtained from the monodromy matrix, we need to calculate the monodromy matrix from the Jacobian matrix.

Assuming that the condition for the periodic trajectory (17) is satisfied by the polynomial approximation with sufficient accuracy, we can obtain the monodromy matrix $\boldsymbol{M}$ from the fundamental matrix $\boldsymbol{V}(T)$, which can be calculated by integrating

$$\dot{\boldsymbol{V}}(t) = \tilde{\boldsymbol{J}}(t)\boldsymbol{V}(t) \tag{28}$$

for one period T from $\boldsymbol{V}(0) = \boldsymbol{I}$. In the numerical calculation, each component of $\tilde{\boldsymbol{J}}(t)$ is approximated as $\tilde{\boldsymbol{J}}_{jk}(t) \simeq \boldsymbol{U}_k(\boldsymbol{p}(t))^\top \boldsymbol{\zeta}_j$. Also, we can give $\{\boldsymbol{U}_j(\boldsymbol{p}(t_\ell))\}_{\ell=1}^L$ in advance to reduce the computational cost. We use the fourth-order Runge-Kutta method, where the fundamental matrix is integrated over the time interval of $2\Delta t$ at each time step. We check the Frobenius norm of the fundamental matrix at each time step and, if necessary, renormalize it to avoid divergence during optimization.

In our previous study [28], we could evaluate the two Floquet exponents of the two-dimensional system without calculating the eigenvalues of the monodromy matrix because one of the two exponents is zero and the sum of the exponents can be calculated by integrating the trace of the Jacobian matrix. Therefore, we could formulate a convex optimization problem for the vector field. However, in three or higher dimensional limit-cycle oscillators, we cannot evaluate their Floquet exponents by such a method because we have only two conditions for the three or more exponents, and they should be calculating fully numerically by evaluating the monodromy matrix. Therefore, even though our aim in this study is to straightforwardly generalize the method to higher dimensions, the resulting optimization problem for the vector field is not longer convex and therefore more difficult to formulate than the two-dimensional case.

C. Optimization Problem

Before formulating the optimization problem, we perform centering and scaling of the vector $\boldsymbol{\xi}$ to facilitate finding the solution. The objective function can be rewritten as $\frac{1}{2}\|\tilde{\boldsymbol{\xi}}\|^2$ by $\tilde{\boldsymbol{\xi}} = \boldsymbol{S}\boldsymbol{\xi} - \bar{\boldsymbol{\xi}}$, where $\boldsymbol{S} \in \mathbb{R}^{NP\times NP}$ is the Cholesky factor of $\boldsymbol{A}^\top\boldsymbol{A} + \gamma\boldsymbol{I}$ and $\bar{\boldsymbol{\xi}}$ is the solution of Eq. (25). We note that optimization is performed on $\tilde{\boldsymbol{\xi}}$, while in calculating the monodromy matrix, we use $\boldsymbol{\xi}$ instead of $\tilde{\boldsymbol{\xi}}$.

The optimization problem is finally formulated as

$$\begin{aligned} \hat{\boldsymbol{\xi}} &= \operatorname*{argmin}_{\tilde{\boldsymbol{\xi}}} \frac{1}{2}\left\|\tilde{\boldsymbol{\xi}}\right\|^2 \\ \text{s.t.} \quad & \lambda_1 = 0, \quad \mathrm{Re}\ \lambda_j \le \lambda_{\mathrm{tol}}, \quad j = 2, \dots, N. \end{aligned} \tag{29}$$

In numerical implementation, the constraint $\lambda_1 = 0$ should be treated as $\mathrm{Re}\ \lambda_1 = 0$ and $\mathrm{Im}\ \lambda_1 = 0$ to avoid λ_1 being a complex value.

Although the objective function is quadratic, the optimization problem is generally non-convex because the feasible region can be complex. We choose the first initial point as $\tilde{\boldsymbol{\xi}} = 0$ because the objective function is quadratic. If the optimization fails for this initial point, we should choose another initial point near $\tilde{\boldsymbol{\xi}} = 0$ and try again. If we could find an optimal solution, we should also confirm that the vector field constructed from the optimal solution has the prescribed stable trajectory and PSF.

V. RESULTS

A. Reconstruction of the Rössler Oscillator

First, we show that it is possible to design a limit-cycle oscillator that has the same periodic trajectory and PSF as the existing oscillator. We consider the Rössler oscillator [5],

$$\frac{d}{dt}\begin{bmatrix} x_1 \\ x_2 \\ x_3 \end{bmatrix} = \begin{bmatrix} -x_2 - x_3 \\ x_1 + a x_2 \\ b + x_3(x_1 - c) \end{bmatrix}, \tag{30}$$

where $a = 0.1$, $b = 0.1$, and $c = 2.4$. This oscillator has a limit cycle with a period $T = 5.9546$ and natural frequency $\omega = 1.0552$. The Floquet exponents are calculated as $\lambda_1 \simeq 0$, $\lambda_2 = -0.9445$, and $\lambda_3 = -1.3166$ from the monodromy matrix and the PSF is calculated by the adjoint equation.

In designing the vector field, we set the time interval as $\Delta t = 2\times10^{-4}$, the maximum order of polynomials as $n = 5$, the weight of regularization as $\gamma = 10^{-7}$, and the tolerance value of stability as $\lambda_{\mathrm{tol}} = -1$, which is smaller than λ_2 of the Rössler oscillator. The designed oscillator has a period $T = 5.9546$ and natural frequency $\omega = 1.0552$, which are almost identical to the original values. The Floquet exponents of the designed oscillator are calculated as $\lambda_1 \simeq 0$, $\lambda_2 = -1.1270 + 0.5276i$, and $\lambda_3 = -1.8667 + 0.5276i$, where i denotes the imaginary unit. Here, λ_2 and λ_3 correspond to the negative real eigenvalues of the monodromy matrix, whose imaginary part is π/T. The real parts of λ_2 and λ_3 are below the given λ_{tol}.

As shown in Fig. 1, the original and designed oscillators have almost identical limit cycles [(a)], velocities on the limit cycle [(b1)-(b3)], and PSFs [(c1)-(c3)]. Although the second Floquet vectors of the Rössler oscillator are real, those of the designed oscillator are complex because the second eigenvalue λ_2 is complex. Similar results were obtained also for the third Floquet vectors. This indicates that we can design an oscillator with distinct properties (i.e., complex Floquet exponents) from the original oscillator, while keeping the same periodic trajectory and PSF as the original oscillator.

B. Design of Artificial Oscillators

Next, we design two types of three-dimensional limit-cycle oscillators with the same artificial periodic trajectory but with different PSFs. We assume that both oscillators have the following periodic trajectory of period $T = 2\pi$ and $\omega = 1$:

$$\boldsymbol{p}(t) = \begin{bmatrix} \cos(t) & \sin(t) & \frac{1}{3}\cos(3t) \end{bmatrix}^\top. \tag{31}$$

The PSF of the first oscillator is assumed as

$$\tilde{\boldsymbol{Z}}_{\mathrm{first}}(t) = \begin{bmatrix} \sin(3t) \\ 2\cos(t) + \sin(3t) - \cos(3t) \\ \cos(t) \end{bmatrix}. \tag{32}$$

We set the data length as $L = 4\times10^3$, the maximum order of polynomials as $n = 5$, the weight of regularization as $\gamma = 10^{-4}$, and the tolerance value of stability as $\lambda_{\mathrm{tol}} = -1$. The designed oscillator has a period $T = 6.2832$ and

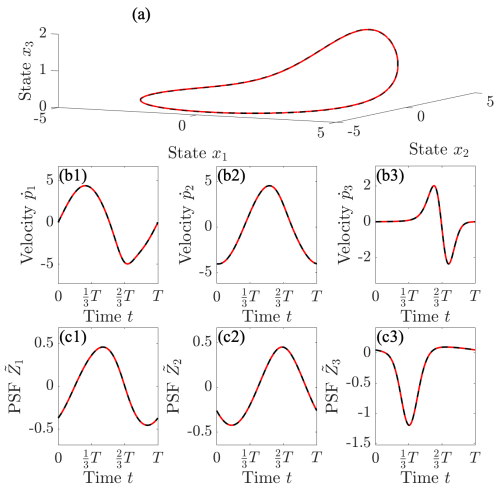

Fig. 1. Designed oscillator with the periodic trajectory and PSF of the Rössler oscillator. (a) Periodic trajectory. (b1)-(b3) Velocity on the limit cycle (x_1-x_3 components). (c1)-(c3) PSF (x_1-x_3 components). In all figures, the red line shows the result of the designed oscillator and the black line shows the original functions.

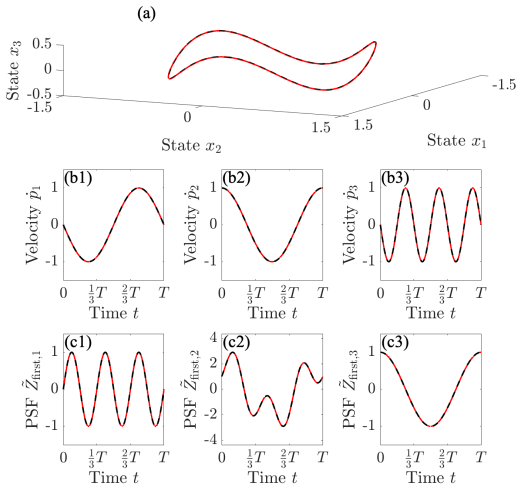

Fig. 2. The first designed oscillator with $\tilde{\boldsymbol{Z}}_{\mathrm{first}}$. (a) Periodic trajectory. (b1)-(b3) Velocity on the limit cycle (x_1-x_3 components). (c1)-(c3) PSF (x_1-x_3 components). In all figures, the red line is the designed one and the black line is the assumed one.

natural frequency $\omega = 1.0000$, which are almost identical to the assumed values. The Floquet exponents of the designed oscillator are calculated as $\lambda_1 \simeq 0$, $\lambda_2 = -1.2240 + 0.0931i$, and $\lambda_3 = -1.2240 - 0.0931i$, where the real parts of λ_2 and λ_3 are below λ_{tol}. As shown in Fig. 2, the designed oscillator has almost the same limit cycle [(a)], velocities [(b1)-(b3)], and PSFs [(c1)-(c3)] as the assumed oscillator.

The PSF of the second oscillator is assumed as

$$\tilde{\boldsymbol{Z}}_{\mathrm{second}}(t) = \begin{bmatrix} -\sin(t) \\ -\sin(3t) + \cos(t) \\ -\cos(t) \end{bmatrix}. \tag{33}$$

We designed the vector field under the same conditions as the first oscillator but with a different value of γ, $\gamma = 10^{-5}$. The designed oscillator has a period $T = 6.2832$ and natural frequency $\omega = 1.0000$, which are also almost identical to the assumed values. The Floquet exponents of the designed oscillator are calculated as $\lambda_1 \simeq 0$, $\lambda_2 = -1.0930 + 0.2311i$, and $\lambda_3 = -1.0930 - 0.2311i$, where the real parts of λ_2 and λ_3 are below λ_{tol}. As shown in Fig. 3, the designed oscillator has almost the same limit cycle [(a)], velocities [(b1)-(b3)], and PSFs [(c1)-(c3)] as the assumed oscillator.

C. Synchronization Dynamics with Different PSFs

We assume that the periodic input to the oscillator is given by $\boldsymbol{q}(t) = [-\cos(3t) + \cos(t),\ 0,\ 0]^{\top}$. Both PSFs satisfy $\boldsymbol{Z}(\theta(t)) = \tilde{\boldsymbol{Z}}(t)$ because $\omega = 1$, and the frequency of the input is assumed to be $\Omega = \omega = 1$. First, if the PSF is $\boldsymbol{Z} = \boldsymbol{Z}_{\mathrm{first}}$, the dynamics of the phase difference $\phi_{\mathrm{first}}(t) = \theta(t) - \Omega t$ is described by

$$\dot{\phi}_{\mathrm{first}} = \varepsilon \Gamma_{\mathrm{first}}(\phi_{\mathrm{first}}) = -\frac{\varepsilon}{2}\sin(3\phi_{\mathrm{first}}), \tag{34}$$

whose PCF is shown in Fig. 4(a1). There are three stable phase-locking points at $\phi_0 = -\frac{2}{3}\pi$, 0, and $\frac{2}{3}\pi$. If the PSF

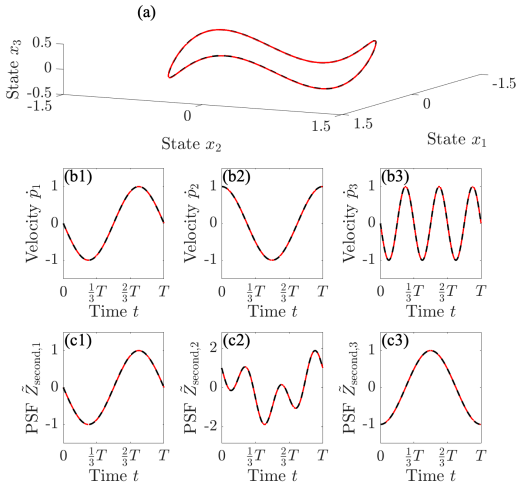

Fig. 3. The second designed oscillator with $\tilde{\boldsymbol{Z}}_{\mathrm{second}}$. (a) Periodic trajectory. (b1)-(b3) Velocity on the limit cycle (x_1-x_3 components). (c1)-(c3) PSF (x_1-x_3 components). In all figures, the red line is the designed one and the black line is the assumed one.

is $\boldsymbol{Z} = \boldsymbol{Z}_{\mathrm{second}}$, the dynamics of $\phi_{\mathrm{second}}(t) = \theta(t) - \Omega t$ is described by

$$\dot{\phi}_{\mathrm{second}} = \varepsilon \Gamma_{\mathrm{second}}(\phi_{\mathrm{second}}) = -\frac{\varepsilon}{2}\sin(\phi_{\mathrm{second}}), \tag{35}$$

whose PCF is shown in Fig. 4(a2). For this PCF, the stable phase-locking point is only $\phi_0 = 0$, which is globally stable. We note that, since the PSF gives the gradient of the asymptotic phase, the asymptotic phases of the two designed oscillator are different. However, the phase defined on the limit cycle is the same for both cases.

We first consider an uncoupled population of 50 oscillators with the PSF $\boldsymbol{Z}_{\mathrm{first}}$ driven by the periodic input $\boldsymbol{q}(t)$, which are initially distributed randomly on the limit cycle. We

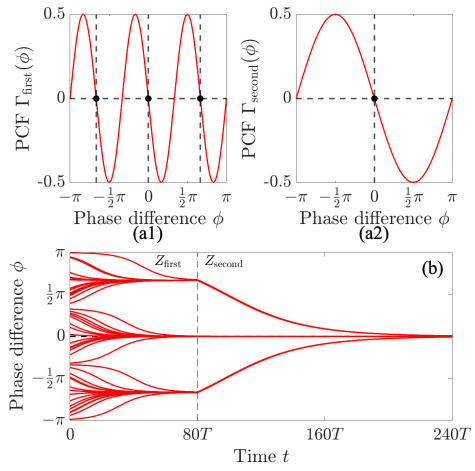

Fig. 4. (a1) PCF $\Gamma_{\rm first}(\phi)$ for the oscillator with $\boldsymbol{Z}_{\rm first}$. (a2) PCF $\Gamma_{\rm second}(\phi)$ for the oscillator with $\boldsymbol{Z}_{\rm second}$. (b) Time evolution of the relative phases of 50 oscillators. For $0 \leq t < 80T$, they obey the phase equation (34) and for $t \geq 80T$, they obey the phase equation (35).

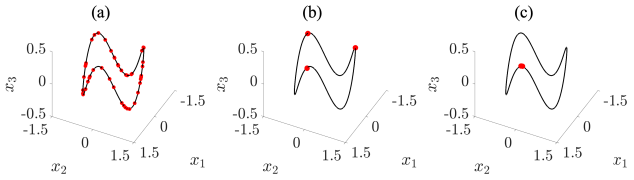

Fig. 5. Direct numerical simulation of 50 uncoupled oscillators obeying Eq. (3), where the PSF is changed from $\boldsymbol{Z}_{\rm first}$ to $\boldsymbol{Z}_{\rm second}$ at $t = 80T$. (a) $t = 0$. (b) $t = 80T$. (c) $t = 240T$.

performed numerical simulations of the evolution of the oscillator states by Eq. (3) and the phase difference by Eqs. (34) and (35). We assumed the intensity of the input to be $\varepsilon = 10^{-2}$ and the time interval to be $\Delta t = \pi/500$. Both the oscillator states and the phase differences converged to the three fixed points before $t = 80T$ as shown in Fig. 4(b) and Figs. 5(a) and 5(b), respectively.

At $t = 80T$, we changed the vector field of all the oscillators from that with the PSF $\boldsymbol{Z}_{\rm first}$ to that with the PSF $\boldsymbol{Z}_{\rm second}$ while driving them by the same $\boldsymbol{q}(t)$. As shown in Figs. 4(b) and 5(c), the oscillators converged to the single fixed point as the PSF is changed. This result clearly shows that the synchronization characteristics of the oscillator, determined by the PSF of the oscillator, can differ even if the periodic trajectory and input are the same.

VI. CONCLUSIONS

We proposed a method for designing stable limit-cycle oscillators with prescribed periodic trajectories and PSFs in general dimensions. We designed an oscillator with the periodic trajectory and PSF of an existing oscillator and showed that the designed one can possess different dynamical properties even if it has the same prescribed conditions. We further designed two oscillators with the same periodic trajectory but with different PSFs and showed that synchronization dynamics can drastically change depending on the PSF even under the same input. Designing limit-cycle oscillators with prescribed PSFs would be beneficial in practical applications. For example, we can design the PCFs to realize desired synchronization dynamics of the oscillators as shown in Sec. V C. Also, we can realize fast synchronization by designing oscillators with the optimal PSF for synchronization performance as described in [34]. Applications of the proposed method to real-world systems will be considered in our future work.

REFERENCES

[1] M. Jouaiti, L. Caron, and P. Hénaff, "Hebbian plasticity in CPG controllers facilitates self-synchronization for human-robot handshaking," Frontiers in Neurorobotics, vol. 12, p. 29, 2018.

[2] F. Dörfler and F. Bullo, "Synchronization and transient stability in power networks and nonuniform Kuramoto oscillators," SIAM Journal on Control and Optimization, vol. 50, no. 3, pp. 1616–1642, 2012.

[3] A. Daryoush, "Optical synchronization of millimeter-wave oscillators for distributed architecture," IEEE Transactions on Microwave Theory and Techniques, vol. 38, no. 5, pp. 467–476, 1990.

[4] D. Wilson and J. Moehlis, "Spatiotemporal control to eliminate cardiac alternans using isostable reduction," Physica D: Nonlinear Phenomena, vol. 342, pp. 32–44, 2017.

[5] S. H. Strogatz, Nonlinear Dynamics and Chaos. Boca Raton: CRC Press, 2015.

[6] Y. Kuramoto, Chemical Oscillations, Waves, and Turbulence. Berlin: Springer, 1984.

[7] A. Pikovsky, M. Rosenblum, and J. Kurths, Synchronization: A universal concept in nonlinear science. Cambridge University Press, 2001.

[8] F. C. Hoppensteadt and E. M. Izhikevich, Weakly Connected Neural Networks. New York: Springer, 1997.

[9] A. T. Winfree, The Geometry of Biological Time. New York: Springer, 2001.

[10] E. Brown, J. Moehlis, and P. Holmes, "On the phase reduction and response dynamics of neural oscillator populations," Neural Computation, vol. 16, no. 4, pp. 673–715, 2004.

[11] G. B. Ermentrout and D. H. Terman, Mathematical Foundations of Neuroscience. New York: Springer, 2010.

[12] H. Nakao, "Phase reduction approach to synchronisation of nonlinear oscillators," Contemporary Physics, vol. 57, no. 2, pp. 188–214, 2016.

[13] Y. Kuramoto and H. Nakao, "On the concept of dynamical reduction: the case of coupled oscillators," Philosophical Transactions of the Royal Society A: Mathematical, Physical and Engineering Sciences, vol. 377, no. 2160, p. 20190041, 2019.

[14] D. Kuelbs, J. Dunefsky, B. Monga, and J. Moehlis, "Analysis of neural clusters due to deep brain stimulation pulses," Biological Cybernetics, vol. 114, no. 6, pp. 589–607, Dec 2020.

[15] A. Zlotnik, Y. Chen, I. Z. Kiss, H.-A. Tanaka, and J.-S. Li, "Optimal waveform for fast entrainment of weakly forced nonlinear oscillators," Phys. Rev. Lett., vol. 111, p. 024102, 2013.

[16] V. Novičenko, "Delayed feedback control of synchronization in weakly coupled oscillator networks," Phys. Rev. E, vol. 92, p. 022919, 2015.

[17] N. Watanabe, Y. Kato, S. Shirasaka, and H. Nakao, "Optimization of linear and nonlinear interaction schemes for stable synchronization of weakly coupled limit-cycle oscillators," Phys. Rev. E, vol. 100, p. 042205, 2019.

[18] B. Monga, D. Wilson, T. Matchen, and J. Moehlis, "Phase reduction and phase-based optimal control for biological systems: a tutorial," Biological cybernetics, vol. 113, no. 1, pp. 11–46, 2019.

[19] B. Monga and J. Moehlis, "Phase distribution control of a population of oscillators," Physica D: Nonlinear Phenomena, vol. 398, pp. 115–129, 2019.

[20] Y. Kato, A. Zlotnik, J.-S. Li, and H. Nakao, "Optimization of periodic input waveforms for global entrainment of weakly forced limit-cycle oscillators," Nonlinear Dynamics, vol. 105, no. 3, pp. 2247–2263, 2021.

[21] S. Takata, Y. Kato, and H. Nakao, "Fast optimal entrainment of limit-cycle oscillators by strong periodic inputs via phase-amplitude reduction and Floquet theory," Chaos: An Interdisciplinary Journal of Nonlinear Science, vol. 31, no. 9, p. 093124, 2021.

[22] M. Ajallooeian, M. N. Ahmadabadi, B. N. Araabi, and H. Moradi, "Design, implementation and analysis of an alternation-based central pattern generator for multidimensional trajectory generation," Robotics and Autonomous Systems, vol. 60, no. 2, pp. 182–198, 2012.
[23] V. Pasandi, H. Sadeghian, M. Keshmiri, and D. Pucci, "An integrated programmable CPG with bounded output," IEEE Transactions on Automatic Control, vol. 67, no. 9, pp. 4658–4673, 2022.
[24] A. J. Ijspeert, J. Nakanishi, H. Hoffmann, P. Pastor, and S. Schaal, "Dynamical movement primitives: Learning attractor models for motor behaviors," Neural Computation, vol. 25, no. 2, pp. 328–373, 2013.
[25] M. Ajallooeian, J. van den Kieboom, A. Mukovskiy, M. A. Giese, and A. J. Ijspeert, "A general family of morphed nonlinear phase oscillators with arbitrary limit cycle shape," Physica D: Nonlinear Phenomena, vol. 263, pp. 41–56, 2013.
[26] M. Okada, K. Tatani, and Y. Nakamura, "Polynomial design of the nonlinear dynamics for the brain-like information processing of whole body motion," in Proceedings 2002 IEEE International Conference on Robotics and Automation (Cat. No.02CH37292), vol. 2, 2002, pp. 1410–1415.
[27] V. Pasandi, A. Dinale, M. Keshmiri, and D. Pucci, "A data driven vector field oscillator with arbitrary limit cycle shape," in 2019 IEEE 58th Conference on Decision and Control (CDC), 2019, pp. 8007–8012.
[28] N. Namura, T. Ishii, and H. Nakao, "Designing two-dimensional limit-cycle oscillators with prescribed trajectories and phase-response characteristics," 2023, arXiv:2301.07237.
[29] S. Townley, A. Ilchmann, M. Weiss, W. Mcclements, A. Ruiz, D. Owens, and D. Pratzel-Wolters, "Existence and learning of oscillations in recurrent neural networks," IEEE Transactions on Neural Networks, vol. 11, no. 1, pp. 205–214, 2000.
[30] P. Zegers and M. Sundareshan, "Trajectory generation and modulation using dynamic neural networks," IEEE Transactions on Neural Networks, vol. 14, no. 3, pp. 520–533, 2003.
[31] G. Jouffroy, "Design of oscillatory recurrent neural network controllers with gradient based algorithms," in 16th European Symposium on Artificial Neural Networks, 2008, pp. 7–12.
[32] J. Guckenheimer and P. Holmes, Nonlinear oscillations, dynamical systems, and bifurcations of vector fields. New York: Springer, 1983.
[33] J. Zhou, "Classification and characteristics of Floquet factorisations in linear continuous-time periodic systems," International Journal of Control, vol. 81, no. 11, pp. 1682–1698, 2008.
[34] A. Abouzeid and B. Ermentrout, "Type-II phase resetting curve is optimal for stochastic synchrony," Phys. Rev. E, vol. 80, p. 011911, 2009.